Preprints (www.preprints.org) | NOT PEER-REVIEWED | Posted: 31 March 2022 doi:10.20944/preprints202111.0488.v2

Rapid optical clearing for high-throughput analysis of tumour spheroids

Gency Gunasingh[1]*, Alexander P Browning[2†], Nikolas K Haass[1]

[1] The University of Queensland Diamantina Institute, The University of Queensland, Brisbane, Australia
[2] School of Mathematical Sciences, Queensland University of Technology, Brisbane, Australia

Abstract

Tumour spheroids are fast becoming commonplace in basic cancer research and drug development. Obtaining high-quality data relating to the inner composition of spheroids is important for analysis, yet existing techniques often use equipment that is not commonly available, are expensive, laborious, cause significant size distortion, or are limited to relatively small spheroids. We present a high-throughput method of mounting, clearing, and imaging tumour spheroids that causes minimal size distortion. Spheroids are mounted in an agarose gel to prevent movement, cleared using a solution prepared from commonly available materials, and imaged using confocal microscopy. We find that our method yields high quality two- and three-dimensional images that provide information about the inner structure of spheroids.

Introduction

Three-dimensional cell cultures, such as spheroids, provide biologically realistic and reproducible models of aggregate cell growth (Hirschhaeuser et al., 2010; Beaumont et al. 2015). These models are fast becoming commonplace in both basic research and drug development, where differences in spheroid size and structure are examined between treatments to ascertain drug efficacy (Smalley et al., 2008, Spoerri et al., 2021a). In these contexts, the ability to collect detailed information from a large number of spheroids is highly advantageous, both from a statistical power perspective, and to allow rapid assessment of cell behaviour across several treatments.

Current techniques for obtaining detailed microscopy images of spheroid structure are either time-consuming, expensive, or produce poor quality images that do not retain key quantitative features such as spheroid size (Nürnberg et al., 2020; Spoerri et al., 2021a). Histological techniques based upon cryosectioning can provide high-quality images but are often time-consuming or utilise materials that are not readily available (Kabadi et al., 2015). The same applies to elegant technologies, such as single plane illumination microscopy (SPIM) (Spoerri et al., 2021b) and multiphoton microscopy (Haass et al., 2014). Modern microscopy technologies have relatively recently enabled so-called optical sectioning, where spheroids are placed within a refractive index matched clearing solution and images obtained using confocal microscopy (Nürnberg et al., 2020; Spoerri et al., 2021a). While these techniques have the potential to produce a high -yield, common

* g.gunasingh@uq.edu.au
† ap.browning@icloud.com

problems include spheroid movement, size distortion and high expense of proprietary clearing solutions. Furthermore, many existing protocols apply only to relatively small spheroids, of less than 300 µm in diameter, limiting the technology to the early stages of tumour growth.

We present a novel protocol that allows high-throughput, high-yield collection of detailed spheroid images using a low-cost refractive index-matched clearing solution (Tainaka et al., 2014; Lloyd-Lewis et al., 2016). To prevent spheroid movement during imaging and provide structural support to reduce size distortion, we first mount spheroids in agarose-PBS gel in a 24-well #1.5 glass bottom plate. Since our technique allows for multiple spheroids to be mounted in each well in a 24-well plate, we can rapidly mount and image large numbers of spheroids across a variety of experimental conditions. To optically clear mounted spheroids and the surrounding gel, we introduce a refractive-index-matched clearing solution constructed from readily available consumables. After a settling period of 24 hours, our protocol provides high-quality 2D and 3D images of spheroid structure, even for relatively large spheroids (approximately 700 µm in diameter), with less than 2% size distortion.

Protocol

Materials and consumables

- Agarose gel (200 µL per 10 spheroids (1 well)).
  - Low-melting agarose powder (2% w/v).
  - PBS (98% w/v).
- Clearing solution.
  - Urea (22% w/w).
  - Quadrol® (9% w/w).
  - Sucrose (44% w/w)
  - Triton X-100 (0.1% w/w)
  - MilliQ water (24.9% w/w)
- Mounting materials.
  - 500 µL clear PCR tubes (1 per well).
  - #1.5 glass bottom 24-well plate.
- Equipment
  - Microwave
  - Heating block
  - Quickspin minifuge

Preprints (www.preprints.org) | NOT PEER-REVIEWED | Posted: 31 March 2022 doi:10.20944/preprints202111.0488.v2

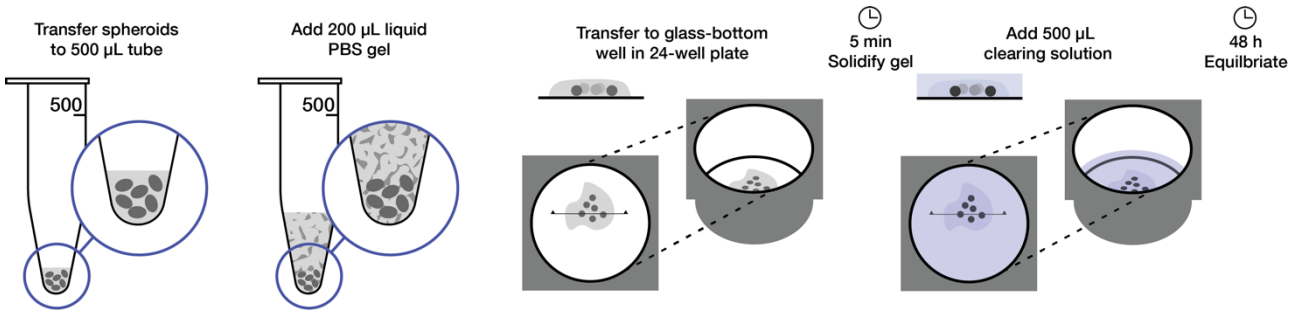

Figure 1. Fixed and stained spheroids are transferred to a 500 µL tube, excess fluid is replaced by 200 µL PBS-based gel and centrifuged. Spheroids are then transferred to a glass-bottom well in a 24-well plate. After gel is allowed to solidify, 500 µL clearing solution is added and spheroids are allowed to equilibrate.

Methods

Methods describe preparation of a sufficient quantity to mount one 24-well plate (approximately 240 spheroids) at 200 µL agarose gel per well, 500 µL clearing solution per well. Methods are illustrated in Fig. 1.

PBS gel preparation

1. Dissolve 0.5 g low-melting agarose in 25 mL phosphate buffered saline (PBS) by boiling in a microwave for 30 s – 1 min with swirling. Ensure agarose is fully dissolved and the solution does not boil over.
2. Gel can be stored at room temperature; check volume before use to account for evaporation. Bring to liquid state (microwave; 20 s – 1 min, with swirling) before using.

Clearing solution preparation

Weigh Quadrol® and adjust the weight of other components to obtain desired concentrations. Weigh desired quantities of all components of the clearing reagent, including water, and heat up the solution in 56°C water bath with constant mixing. Once mixed, degas the solution or allow the bubbles to rise to surface prior to use. The solution is stable at room temperature up to 2 months.

Mounting

1. Transfer fixed and stained spheroids to 500 µL PCR tubes at one tube per condition (approximately 10 spheroids). Let spheroids gravity settle to bottom of the tube.
2. Replace solution with 200 µL liquid agarose gel and centrifuge for 30 s. Unless mounting immediately, place in heating block at 50 °C to avoid gel hardening.
3. Aspirate spheroids in ~50 µL liquid agarose gel. Dispense in well of a 24-well glass bottom plate. Before gel hardens, separate spheroids using pipette tip in surrounding gel, and ensure spheroids are covered with gel. Optionally, place plate on ice to rapidly set gel.
4. Add 500 µL clearing solution per well, ensuring gel is submerged. Leave for > 24 h before imaging.

Preprints (www.preprints.org) | NOT PEER-REVIEWED | Posted: 31 March 2022 doi:10.20944/preprints202111.0488.v2

Imaging

1. Choose an objective that has a working distance long enough to encompass the entire spheroid including the mounting height of the spheroid in the vessel.
2. For equatorial section, adjust focus till the largest surface area is reached in the XY plane and image with required laser power, detector voltage, gain and offset settings.
3. For 3D images, set start and end of the spheroids, choose appropriate signal intensity at various Z-depth using Z intensity correction settings (Bright Z in FV3000) before imaging.
4. For best image resolution, use Nyquist sampling rate for X, Y and Z.

All images shown in this paper were imaged using an Olympus FLUOVIEW FV3000 confocal microscope.

Representative results

To demonstrate the ability of our clearing method to provide high-quality two- and three-dimensional images, we mount, clear and image relatively large spheroids (Fig. 2) grown from human melanoma cell lines according to methods given in Spoerri et al., 2017. All microscopy files are provided on GitHub (see Data Availability). Compared with PBS-mounted spheroids, the clearing solution provides high-clarity images with minimal size distortion (Fig. 2a). The protocol allows for high-resolution imaging of cell-level details without histological sectioning; this cross-sectional image was obtained from a 20x air objective (Olympus UPlanSApo) at a resolution of 4096 x 4096 px without stitching (Fig. 2b). Using a lower magnification and lower numerical aperture (NA) objective with longer working distance, we demonstrate three-dimensional confocal images that provide cell-level detail at a depth of at least 200 µm (Fig. 2c). Note that Bright-Z in FV3000, which provides a depth-based intensity correction in Z, allows the imaging of the whole spheroid. We note that light-scattering due to the necrotic core limits our ability to image the far side of the spheroid. Deeper penetration and less scattering of a far-red fluorophore, such as DRAQ7 nuclear stain, allows for even further improved three-dimensional spheroid structure representation (Fig. 3). Thinner Z-slice may allow for better Z-resolution but this significantly increases the imaging time and photobleaching of the fluorophores.

To determine whether the clearing solution causes size distortion, we image 12 spheroids in PBS gel, and 6 h, 12 h, 24 h, 72 h and 168 h following the introduction of the clearing solution. We summarise images by determining the diameter of the spheroid, defined based on a sphere with the same cross-sectional area as the spheroid (Fig. 4a). While the spheroids are observed to slightly increase in size over the first 6 h, indicated by a diameter fold-change of between –2% and 6% (Fig. 4b), after 24 to 72 h the spheroids return to a size approximately equal to the corresponding size in PBS gel only (Fig. 4c). Combined with automated image processing (Browning et al., 2021a) and minimal size distortion, our high-throughput protocol lends to

Preprints (www.preprints.org) | NOT PEER-REVIEWED | Posted: 31 March 2022 doi:10.20944/preprints202111.0488.v2

quantitative analysis of spheroid inner structure (Browning et al., 2021b, Murphy et al., 2022, Klowss et al., 2022).

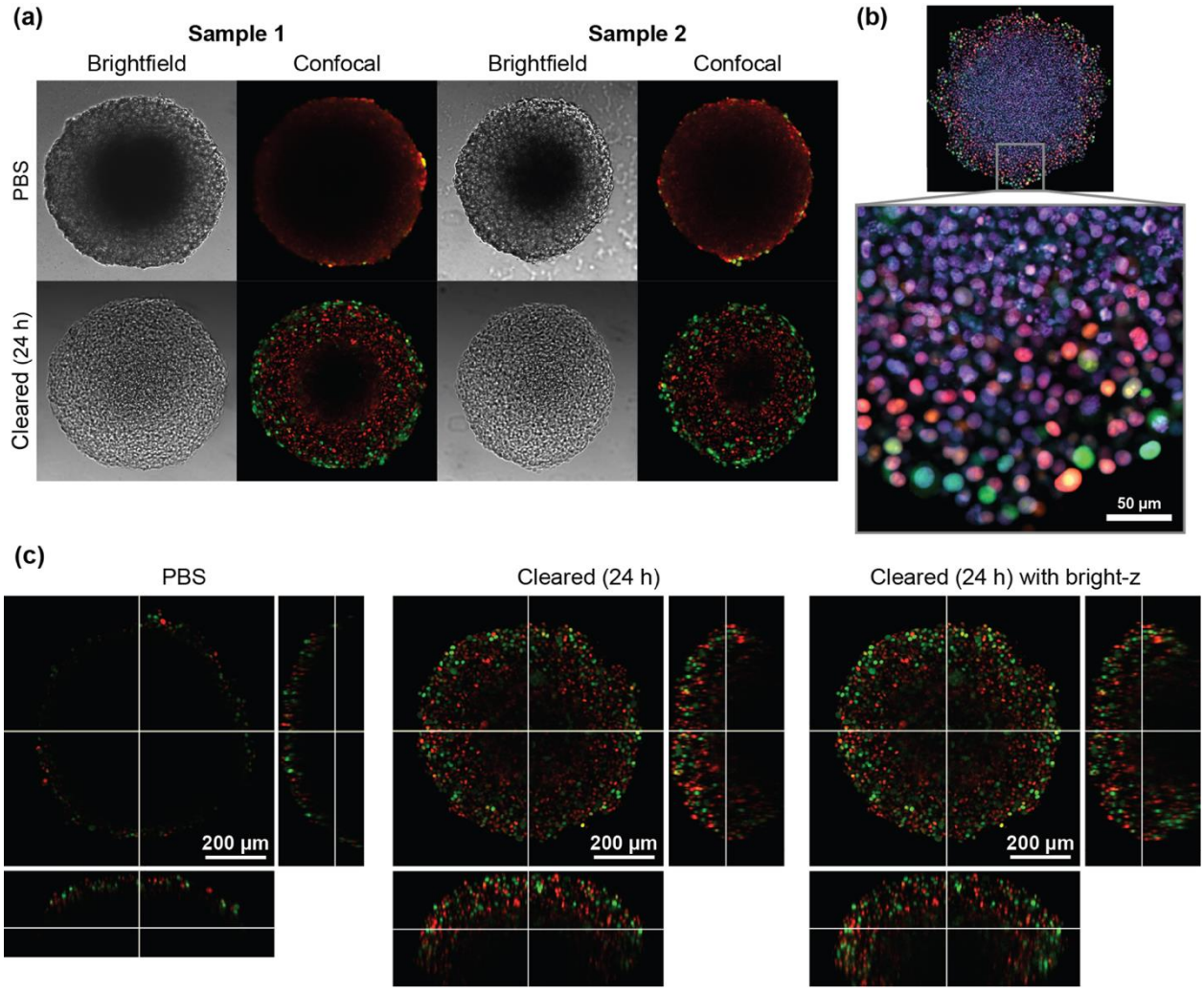

Figure 2. Confocal cross-sectional images obtained of spheroids grown from human melanoma cells transduced with fluorescent cell cycle indicators (FUCCI) (Sakaue-Sawano et al., 2008; Haass et al., 2014). Spheroids are grown using methods described in Spoerri et al. 2017. Colouring indicates cell nuclei positive for mKO2 (red), which indicates cells in gap 1; and cell nuclei positive for mAG (green), which indicates cells in gap 2. **(a)** Spheroids grown from 5000 FUCCI-WM983b cells (Haass et al., 2014), harvested at day 10 and imaged in PBS gel and 24 h after clearing solution is added. Comparing brightfield and confocal images before and after clearing solution shows minimal size distortion, and a large gain in clarity. Images are obtained using a 10x objective. **(b)** Spheroid grown from FUCCI-WM164 cells (Haass et al., 2014) permeabilised using Triton and stained with DRAQ7, which stains all cell nuclei. Image is obtained using a 20x objective, demonstrating the clearing solution allows high-resolution imaging of cell-level details. **(c)** Three-dimensional images (10x) obtained of FUCCI-WM164 spheroids in PBS and 24 h after clearing solution is added. We apply bright-z to adjust exposure settings for cross-sections obtained deeper inside the spheroid. Cleared images still show light loss due to scattering from the necrotic core.

Preprints (www.preprints.org) | NOT PEER-REVIEWED | Posted: 31 March 2022 doi:10.20944/preprints202111.0488.v2

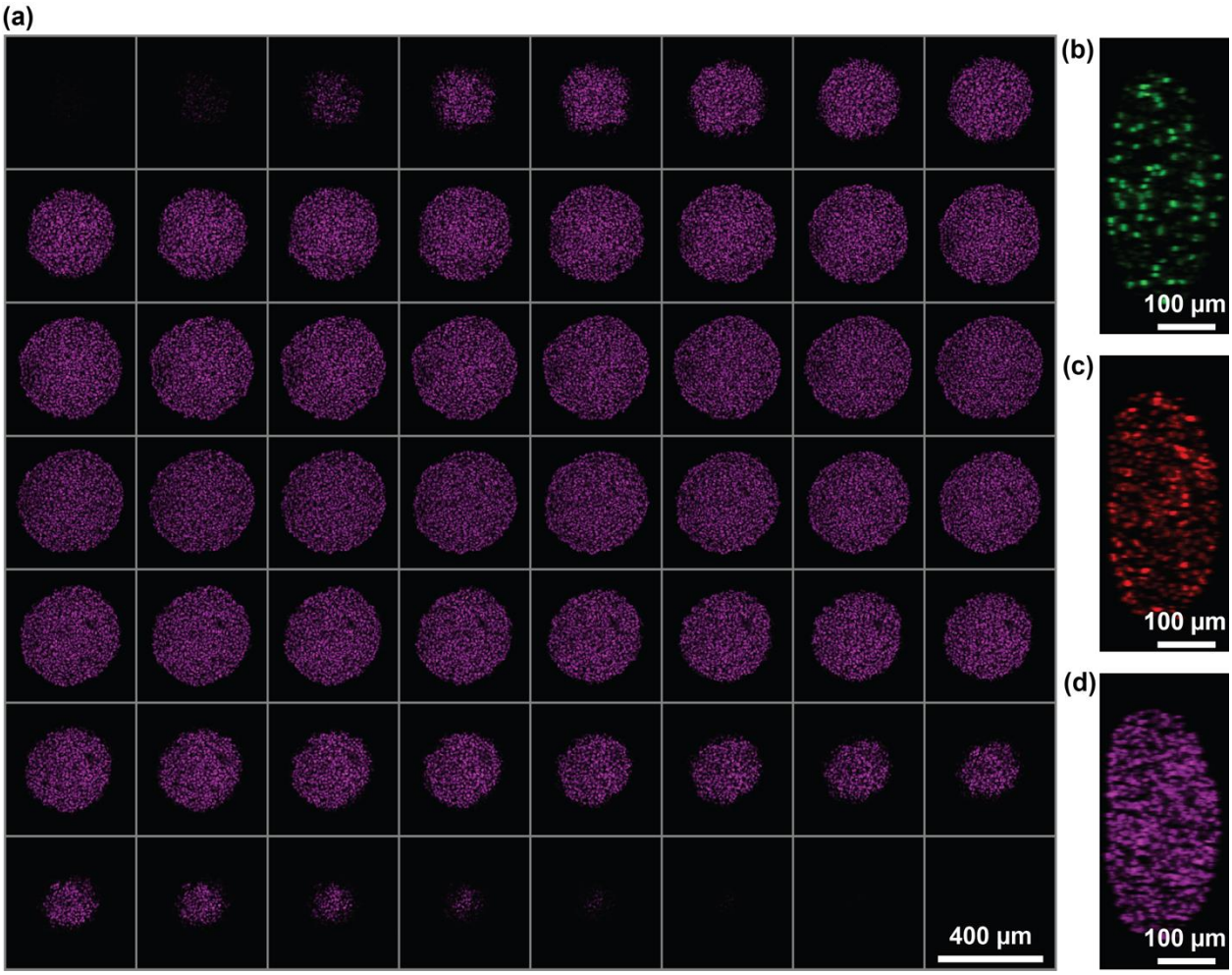

Figure 3. Confocal microscopy images of a FUCCI human melanoma spheroid (Haass et al. 2014) at 10x magnification and lower NA (0.4) allowing for a large z-depth with minimal loss of signal. **(a)** 3.88 µm slices of spheroid nuclei stained with DRAQ7. **(b–d)** YZ resolution in the 488 (FUCCI green), 568 (FUCCI red), and 647 nm (DRAQ7) channels, respectively.

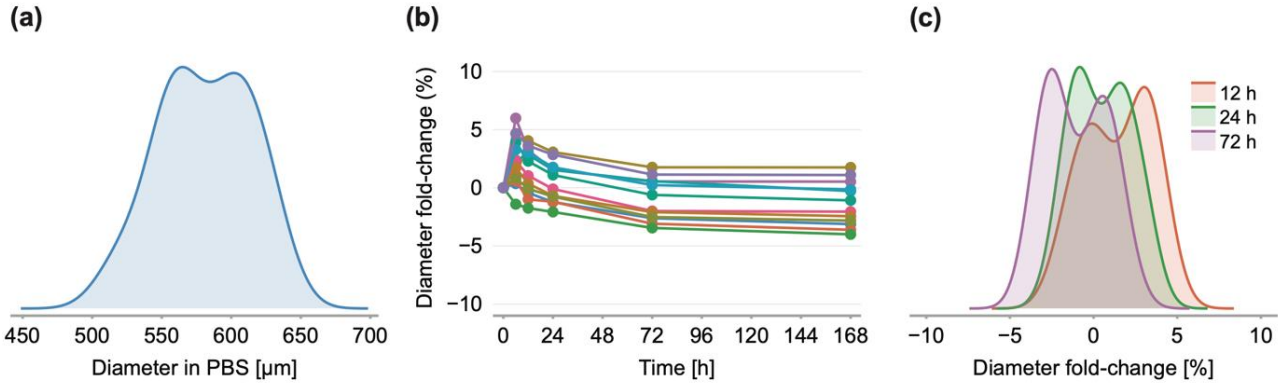

Figure 4. Clearing solution has very little impact on spheroid size. **(a)** Distribution of initial spheroid size (equivalent diameter) in PBS gel (n = 12 spheroids). **(b)** Diameter fold-change over time since addition of clearing solution. At 0 hours, spheroids are in PBS gel only. **(c)** Distribution of diameter fold-changes at 12 h, 24 h and 72 h.

Discussion

We present a high-throughput protocol for obtaining high-quality two- and three-dimensional images of tumour spheroids. Our method uses readily available consumables to mount and clear spheroids that maintains optical clarity and endogenous fluorescence while preventing size distortion. Given that our technique allows multiple spheroids to be mounted simultaneously in a multi-well plate, our protocol is well suited to quantitative analysis pipelines that require spheroid structure information from large numbers of spheroids.

Despite the method allowing for signal detection deeper within the spheroid, fluorophores excited by UV cause significant light scattering which in turn leads to low signal-to-noise ratio. Care must be taken when choosing fluorophores to visualize the target protein. For example, staining less abundant and structural proteins with longer wavelength fluorophores and more abundant protein or nuclear stains with shorter wavelength fluorophores will achieve best result.

We demonstrate that our method allows for better visualisation of cells deep inside the spheroids and, at the same time, does not distort spheroid structure and integrity.

Data availability

Microscopy images and code used to perform spheroid size analysis are available on GitHub at https://github.com/ap-browning/SpheroidMounting.

Acknowledgements

This research was carried out at the Translational Research Institute (TRI), Woolloongabba, QLD. TRI is supported by a grant from the Australian Government. We thank the staff in the microscopy core facility at TRI for their outstanding technical support. We thank Prof. Atsushi Miyawaki, RIKEN, Wako-city, Japan, for providing the FUCCI constructs, Prof. Meenhard Herlyn and Ms. Patricia Brafford, The Wistar Institute, Philadelphia, PA, for providing the cell lines.

This work was supported by project grants to N.K.H.: Australian Research Council (DP200100177) and Meehan Project Grant (021174 2017002565).

Bibliography

Beaumont KA, Anfosso A, Ahmed F, Weninger W, Haass NK. Imaging- and Flow Cytometry-based Analysis of Cell Position and the Cell Cycle in 3D Melanoma Spheroids. *J Vis Exp* **106**, e53486 (2015)

Browning AP & Murphy RJ. Image processing algorithm to identify structure of tumour spheroids with cell cycle labelling. *Zenodo* (2021a)

Browning AP, Sharp JA, Murphy RJ, Gunasingh G, Lawson B, Burrage K, Haass NK & Simpson MJ. Quantitative analysis of tumour spheroid structure. *eLife* **10**, e73020 (2021)

Haass NK, Beaumont KA, Hill DS, Anfosso A, Mrass P, Munoz MA, Kinjyo I & Weninger W. Real-time cell cycle imaging during melanoma growth, invasion, and drug response. *Pigment Cell Melanoma Research* **27**, 764–776 (2014).

Hirschhaeuser, F., Menne, H., Dittfeld, C., West, J. & Mueller-Klieser W. Multicellular tumor spheroids: an underestimated tool is catching up again. *Journal of Biotechnology* **148**, 3–15 (2010).

Ivanov DP & Grabowska AM. Spheroid arrays for high-throughput single-cell analysis of spatial patterns and biomarker expression in 3D. *Scientific Reports* **7**, 41160 (2017).

Kabadi PK, Vantangoli MM, Rodd AL, Leary E & Madnick SJ. Into the depths: techniques for in vitro three-dimensional microtissue visualization. *Biotechniques* **59**, 279–286 (2015).

Klowss JJ, Browning AP, Murphy RJ, Carr EJ, Plank MJ, Gunasingh G, Haass NK, Simpson MJ. A stochastic mathematical model of 4D tumour spheroids with real-time fluorescent cell cycle imaging. *J R Soc Interface* (in press)

Murphy RJ, Browning AP, Gunasingh G, Haass NK, Simpson MJ. Designing and interpreting 4D tumour spheroid experiments. *Communications Biology* **5,** 91 (2022)

Lloyd-Lewis B, Davis FM, Harris OB, Hitchcock JR, Lourenco FC, Pasche M, Watson CJ. Imaging the mammary gland and mammary tumours in 3D: optical tissue clearing and immunofluorescence methods. *Breast Cancer Research* **18**, 127 (2016).

Nürnberg E, Vitacolonna M, Klicks J, von Molitor E & Cesetti T. Routine optical clearing of 3D-cell cultures: simplicity forward. *Frontiers in Molecular Biosciences* **7**, 20 (2020).

Sakaue-Sawano A, Kurokawa H, Morimura T, Hanyu A & Hama H. Visualizing spatiotemporal dynamics of multicellular cell-cycle progression. *Cell* **132**, 487–498 (2008).

Smalley K, Lioni M, Noma K, Haass NK & Herlyn, M. In vitro three-dimensional tumor microenvironment models for anticancer drug discovery. *Expert Opinion on Drug* Discovery **3**, 1–10 (2008).

Spoerri L, Beaumont KA, Anfosso A & Haass NK. Real-time cell cycle imaging in a 3D cell culture model of melanoma. *Methods in Molecular Biology* **1612**, 401-416 (2017).

Spoerri L, Gunasingh G & Haass NK. Fluorescence-based quantitative and spatial analysis of tumour spheroids: a proposed tool to predict patient-specific therapy response. *Frontiers Digital Health* **3**, 668390 (2021).

Spoerri L, Tonnessen-Murray CA, Gunasingh GP, Hill DS, Beaumont KA, Jurek RJ, Chauhan J, Vanwalleghem GC, Fane ME, Daignault-Mill SM, Matigian N, Boyle GM, Scott EK, Smith AG, Stehbens SJ, Schaider H, Gabrielli B, Weninger W, Goding CR, Haass NK. Phenotypic melanoma heterogeneity is regulated through cell-matrix interaction-dependent changes in tumor microarchitecture. *bioRxiv* (2021b)

Tainaka K, Kubota SI, Suyama TQ, Susaki EA, Perrin D, Ukai-Tadenuma M, Ukai H, Ueda HR. Whole-body imaging with single-cell resolution by tissue decolorization. *Cell* **159**, 911–924 (2014).